Journal of Luminescence 169 (2016) 674–677

Contents lists available at ScienceDirect

Journal of Luminescence

journal homepage: www.elsevier.com/locate/jlumin

Scintillation response of Ce^{3+} doped GdGa-LuAG multicomponent garnet films under e-beam excitation

M. Kucera [a,*], Z. Onderisinova [a], J. Bok [b], M. Hanus [a], P. Schauer [b], M. Nikl [c]

[a] Charles University, Faculty of Mathematics and Physics, Ke Karlovu 5, 12116 Prague 2, Czech Republic
[b] Institute of Scientific Instruments, AS CR, Kralovopolska 147, 61264 Brno, Czech Republic
[c] Institute of Physics, AS CR, Cukrovarnicka 10, 16000 Prague 6, Czech Republic

ARTICLE INFO

Article history:
Received 14 October 2014
Received in revised form
11 January 2015
Accepted 13 January 2015
Available online 21 January 2015

Keywords:
Multicomponent garnets
Cathodoluminescence
LuAG:Ce
Scintillation
Liquid phase epitaxy

ABSTRACT

Scintillation properties of multicomponent $(GdLuY)_3(GaAl)_5O_{12}:Ce^{3+}$ epitaxial garnet films were studied under electron beam excitation. The role of the shallow traps was investigated using the scintillation decay kinetics and cathodoluminescence spectroscopy. Tunneling-driven recombination, which provides a physical ground for the slow scintillation decay component in LuAG:Ce single crystals, is discussed in detail.

1. Introduction

Ce^{3+} doped aluminum garnets, YAG:Ce, LuAG:Ce, are prospective scintillation materials for detection of X-rays, gamma rays or high energy particles [1]. Thin single crystalline films have potential application in high resolution imaging screens for electron or X-ray detection [2,3]. The light yield of these garnet materials prepared in the bulk single crystal form from the melt, e.g. by Czochralski technique is, however, degraded by inevitable structural defects, such as antisite defects (AD). They give rise to trap states and appearance of slow light (delayed radiative recombination components) in scintillation decays [4–6]. Recently, it has been shown that due to the combined substitution of Gd and Ga, the shallow traps are extensively suppressed in bulk aluminum garnet crystals [7]. This consequently leads to significant improvement of scintillation efficiency, namely to increase of the LY [8] and improvement of afterglow characteristics [9].

In this work we have studied the scintillation properties of Ce^{3+}-doped multicomponent $(GdYLu)_3(GaAl)_5O_{12}$:Ce garnet single crystalline films under electron beam excitation. The Gd, Ga co-doped LuAG:Ce samples were grown by liquid phase epitaxy. We have concentrated on the role of shallow electron traps. Scintillation decay kinetics measured with large dynamical resolution and in extended time scale provides an insight into the mechanism of delayed recombination in this material.

2. Experimental

2.1. Growth of epitaxial garnet films

The single crystalline epitaxial garnet films were grown by the isothermal dipping liquid phase epitaxy onto YAG and LuAG substrates of (111) crystallographic orientation and 20 mm in diameter. Special care was focused on purity of samples and eliminating potential impurities coming from the flux. Starting raw materials of 5N purity were used. Ce-doped GdYLuGaAl-garnet epitaxial films were grown from lead-free $BaO–B_2O_3–BaF_2$ flux, technical details were published elsewhere [10]. The films grown from the BaO-flux are not contaminated by flux impurities (such as Pb^{2+}), which are known to quench the Ce^{3+} fast 5d–4f emission [11]. The thickness of films was 8–18 μm, the growth temperatures were in the range 1020–1070 °C. The epitaxial films are single crystalline and single phase as corroborated by the XRD [12]. The composition was measured by the EPMA. The set of samples reported in this work comprises reference sample LuAG:Ce, and samples substituted only by Gd ions and those doped simultaneously by Gd and Ga ions. Sample parameters reported in this work are shown in Table 1.

2.2. Optical and scintillation properties

The spectral properties were studied in the range 200–1000 nm using the optical absorption, photoluminescence (PL) and cathodoluminescence (CL) spectroscopies. The PL decay of

* Corresponding author. Tel.: +420 22 191 1329.
E-mail address: kucera@karlov.mff.cuni.cz (M. Kucera).

http://dx.doi.org/10.1016/j.jlumin.2015.01.034
0022-2313/

Table 1
Thickness and composition determined by the EPMA of $(Ce_xY_yGd_zLu_{3-x-y-z})(Al_{5-w}Ga_w)O_{12}$ samples.

Sample	Thickness [μm]	Ce content x	Y content y	Gd content z	Ga content w
12LBC1	12.3	0.009	0	0	0
14LBC1	10.4	0.013	0.44	0.12	0
14LBC4	15.9	0.011	0.38	0.55	1.30
14LBC7	8.0	0.008	0.37	0.96	1.50

5d–4f (Ce^{3+}) emission was excited by nanosecond LED and measured by the time correlated single photon counting method.

The CL spectra were measured under excitation of electron beam with energy of 10 keV and current of 20 nA and the beam spot had 2 mm in diameter. Spectra were collected by Horiba JY iHR320 spectrometer with Synapse CCD back illuminated detector. The data were corrected for the apparatus spectral function. In the CL experiments the samples were coated by 100 nm thick layer of Al. The penetration depth of electrons in the crystal <1 μm [13] thus all energy is deposited in the garnet film and the substrate is not excited.

The CL decays were measured under excitation by an electron beam pulse of 10 keV and 50 nA with pulse duration of 50 ns and repetition rate of 100 Hz. Emission was collected through spectral range of 450–700 nm of Ce^{3+} (5d–4f) emission band. The decays were measured with 2.5 GHz oscilloscope Tektronix DPO7254 with sampling rate of 40 GS/s. High sampling frequency allows to measure the decays in a broad time range up to 40 μs with 5 ns time resolution and with high dynamical resolution of 4 orders of magnitude. This experimental configuration enables to detect simultaneously both fast and slow decay components, which can differ in several orders of magnitude. The decay curves were corrected for the response of the detection unit. The details of the CL apparatus are published in ref. [14]. All measurements were made at room temperature.

3. Results and discussion

3.1. Cathodoluminescence (CL) spectra

The CL spectra of Gd, Ga substituted samples and reference LuAG:Ce sample are displayed in Fig. 1. Several features are worth to be mentioned in more detail as follows:

(a) The intensity of the Ce-related spectral band between 450 and 700 nm increases with Gd and Ga content. Integrated intensity in a sample with the highest Gd and Ga content (14LBC7), is in 60% higher compared to the reference LuAG:Ce sample. This rise of the CL intensity is consistent with intensity increase observed in these samples also in the PL spectra [15] and X-ray excited radioluminescence [16] and points to positive role of Gd, Ga co-doping in luminescence and scintillation mechanism. Furthermore, due to GdGa substitution the Ce^{3+} emission spectral band is broadened and considerably augmented especially towards the red spectral range, i.e. increased emission to the higher energy ground multiplet $^2F_{7/2}$, cf. Fig. 4.

(b) The sharp emission peak at 312 nm originating from slow 4f–4f (Gd^{3+}) transitions, Fig. 1, is very intense especially in samples with low Gd content. With increasing Gd concentration, this peak wanes and at Gd content above ~50% it completely disappears due to the concentration quenching [16]. The Gd emission peak diminishes also due to $Gd^{3+} \rightarrow Ce^{3+}$ energy transfer, as was demonstrated in Refs. [15,16], however, due to limited Ce content in samples, $<0.5\%$, the Gd emission is only partly reduced.

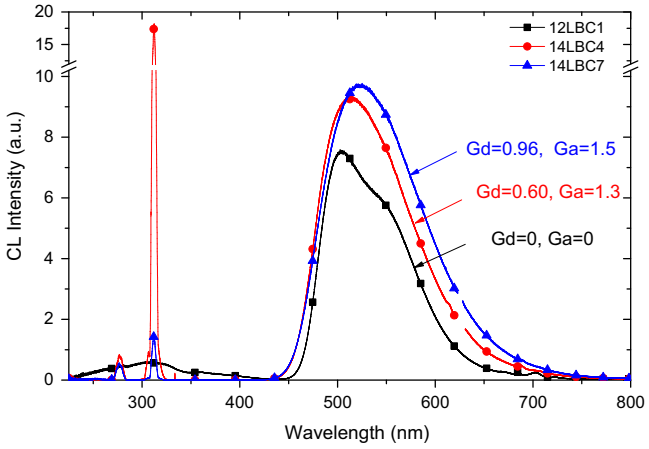

Fig. 1. Cathodoluminescence spectra of $(LuYGd)_3(AlGa)_5O_{12}$:Ce garnet epitaxial films.

(c) In pure LuAG:Ce sample the intrinsic (host) emission band is observed in the range between 200 and 400 nm, sample 12LBC1 in Fig. 1. This broad UV emission is typical for single crystal aluminum garnets LuAG:Ce and YAG:Ce and comes from shallow electrons traps associated with antisite defects Lu_{Al} or Y_{Al} and excitons localized near these defects [4–6]. In epitaxial films this UV emission bands has considerably lower intensity compared to single crystals due to lower content of intrinsic defects in films. Nevertheless, an overlap of the host UV emission and 4f–$5d_2$ (Ce^{3+}) absorption band at 340 nm has negative impact on the decay kinetics and consequently leads to appearance of slower components in the scintillation decay. This intrinsic UV emission is completely suppressed in Gd, Ga co-doped samples as shown in Fig. 1. This is significant advantage of this material system. The mechanism is similar to that observed e.g. in Tb doped YAG [17]: favorable position of Gd absorption states in the UV range promotes the energy transfer from the host lattice to Gd ions which leads, at higher Gd content, to complete quenching of the host emission. Furthermore, because of bandgap reduction due to the Ga substitution, the shallow traps are buried into the conduction band in heavily Ga doped garnets and this is additional effective way for quenching of the UV emission, e.g. [18,19].

3.2. Cathodoluminescence decay kinetics

The CL decay kinetics provides valuable information on defect centers and their influence on scintillation properties. High dynamical and time ranges of decay experiments enabled to carry out precise deconvolution of the experimental curves and reckon fast and slow components simultaneously with sufficient precision.

As an example, in Fig. 2a the scintillation decay curve is displayed in a semi logarithmic scale. The decay is evidently multicomponent – the best fit was obtained only with 4 exponential terms using $I = \sum A_i \exp(-t/\tau_i)$ formula. The fundamental fast component was between 50 and 70 ns in all samples and corresponds to the Ce^{3+}-related 5d–4f emission. Another three slow components were in the range from hundreds of nanoseconds up to 10 μs. Since there is only one emission center in studied garnet systems, namely Ce^{3+}, the interpretation of large number of slower components is disputable and obtained values are rather a consequence of iteration procedure and fitting approach than actual existing centers.

Alternative approach is shown in Fig. 2b, where the decays are displayed in log–log scale. Two contributions are obvious in the curves – namely fast decay observed at $t<300$ ns and a linear part

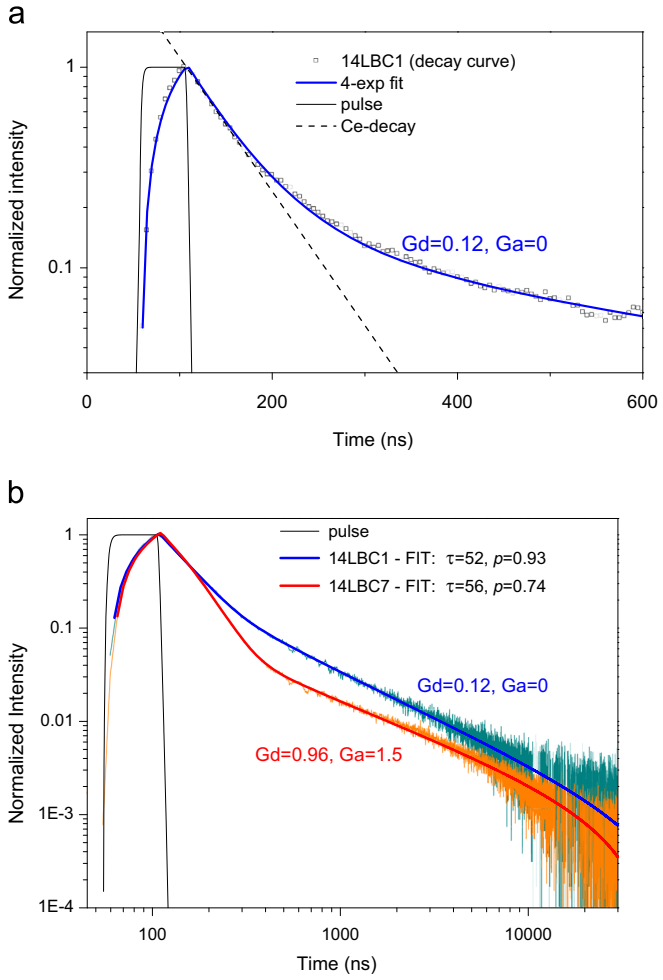

Fig. 2. Cathodoluminescence decays. (a) Initial part of the decay curve in semi-logarithmic scale of low doped LuAG:CeGd sample, solid line – 4-exponential fit, dashed line – fast 51 ns component, (b) one-exponential and power law function fit using Eq. (1) in log–log scale shown in the full experimental time range up to 30 μs for low and medium doped LuAG:CeGd samples. The thick solid lines are convolutions of the decay functions with the excitation pulse.

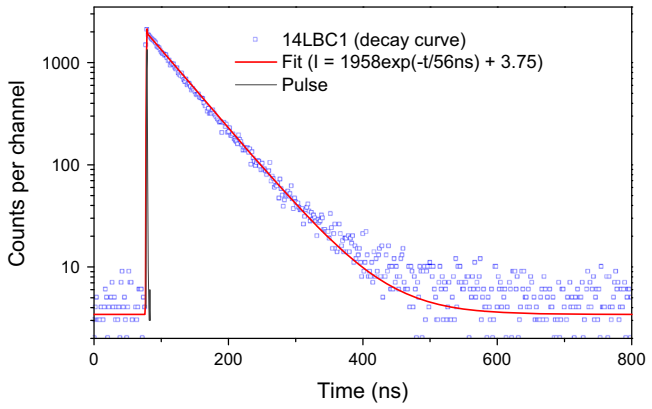

Fig. 3. Photoluminescence decay of 5d–4f (Ce^{3+}) emission measured by time correlated single photon counting at $\lambda_{ex}=339$ nm and $\lambda_{em}=520$ nm. The solid line is convolutions of one-exponential decay function with the excitation pulse.

that follows at longer times. The initial part of the decay at short times comes from Ce^{3+} and is described by an exponential decay as above. The linear part at higher times can be approximated by a power law function, t^{-p}, where p is constant. The model function for fitting experimental decay curves reads

$$I = I_1 \exp(-t/\tau_{Ce}) + I_2 (t_0 - t)^{-p} + I_0, \quad (1)$$

where τ_{Ce} is the intrinsic Ce-related decay time, t_0 compensates for nonzero time of the excitation pulse and I_0 is background signal. The exponential and power function components thus account for the first and second stage in the scintillation decay, respectively. The results of the fit using Eq. 1 for two samples are shown also in Fig. 2b (solid lines). It is evident that just two terms in Eq. (1) provide sufficiently good fit to the entire experimental time range. The first term is evidently the Ce^{3+}-related 5d–4f emission. Single-exponential decay suggests that there is only one emission center, namely Ce^{3+}, as presumed. The obtained scintillation decay time τ_{Ce} was 45 ns in LuAG:Ce and 54–70 ns in Gd, Ga co-doped samples. For comparison the PL decay (excitation at 340 nm and emission at 520 nm) is shown in Fig. 3. The PL decays times are $\tau_{PL}=58$ ns in pure LuAG:Ce and 52–56 ns in GdGa co-doped samples, i.e. the scatter of τ values was significantly lower compared to Ce-related scintillation decay. The PL decays times are close to intrinsic Ce^{3+} value in aluminum garnets. Furthermore, in the PL decay the signal decreases within time interval of 0.5 μs by a factor of ~500 and the decays are strictly single-exponential, however, in the scintillation decay this decrease is only 20–40 × within the same time interval and at longer times the power law function dominates in the decay curves. These observations demonstrate more complicated return of the excited system towards the ground state after excitation by high energy particles/photons.

The power law term, which dominates in the scintillation decays above ~300 ns, is not related to any independent emission center. It was shown by Tachiya and Mozumder [20] and Huntley [21] that tunneling of a trapped electron through a potential barrier to a nearby recombination center can be described by t^{-p} dependence with sufficiently high precision, where constant p is between 0.95 and 1.5. In this approach, both the traps and emission centers are randomly distributed in the crystal lattice. Parameter p depends only on material and for sufficiently deep trap it should not depend on temperature.

The fit of decay curves provided p values of 1.6 in LuAG:Ce and 0.74–1.11 in Gd, Ga co-doped samples. The scatter of obtained values of p comes likely from randomly distributed trap states, which lead to range of trap energies, however, the most probable reason, not considered in the Huntley's model, is thermal ionization of shallow traps, which may occur simultaneously with tunneling. Possible pathways of deexcitation of an electron captured on a virtual trap are shown in Fig. 4. Neglecting radiative or nonradiative recombination from a trap itself (wavy line), we have to take into consideration thermal ionization of a trap center with subsequent capturing of an electron at an empty 5d state of Ce^{4+} creating excited Ce^{3+} center (dashed line) and followed by the delayed radiative recombination from the $5d_1$ state. This delayed emission is, unlike to the tunneling process, strongly temperature dependent described by the Boltzmann factor $\exp(-\Delta E/k_BT)$, where ΔE is the activation energy of the center. The direct tunneling from a trap through an energy barrier to an empty $5d_1$ state of a nearby Ce^{4+} center is symbolized by the thick arrow in Fig. 4. The Ce^{4+} center is created by preceding hole capture at Ce^{3+} ion. It is also worth noting that recent study of low temperature thermoluminescence characteristics in $Gd_3Ga_3Al_2O_{12}$:Ce single crystals [22] suggested that this material contains rather set of discrete traps superposed with wide quasi-continuous distributions of trapping levels, which can explain the observed characteristics quantitatively well as done before considering the tunneling concept [6].

Nevertheless, the quantum tunneling seems to be the most reasonable mechanism which describes slow components in the scintillation decay. It is evident from Fig. 2b, that slow light plays important role in LuAG:Ce. Relative ratio of prompt Ce decay and delayed decay was assessed by integration of the decay curves: the fast Ce-related component carry only smaller part of emission intensity – in LuAG:Ce films it is < 30%, the rest is emitted as slow light. However,

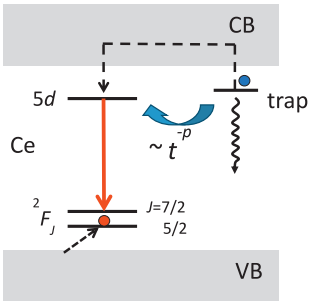

Fig. 4. Sketch of energy levels and possible mechanisms of deexcitation of a trap center. (a) Wavy line – radiative or nonradiative de-excitation of a trap itself; (b) dashed line – thermal ionization of a trap with subsequent capturing of an electron (blue circle at a trap level) at an empty 5d level of Ce^{4+} ion followed by delayed radiative recombination; (c) thick arrow – quantum tunneling through an energy barrier from a trap to a nearby Ce^{4+} activator center. Ce^{4+} center is created by preceding hole capture (red circle at 5/2 level at Ce^{3+} ion. CB – conduction band, VB – valence band. (For interpretation of the references to color in this figure legend, the reader is referred to the web version of this article.)

increasing Gd, Ga content, the situation changes and for sample with higher Gd and Ga content (sample 14LBC7) already 46% of energy is in the fast component. This suggests that the shallow traps, responsible for the tunnel recombination, are significantly reduced in Gd, Ga substituted garnets and support the model in Ref. [19]: the combined effect of Gd, Ga substitution reduces the band-gap and the shallow trap states become buried into the conduction band.

In fact, more experimental work is needed to support above discussions, particularly temperature dependencies of decays and thermally stimulated luminescence, which would enable to assess contributions to the delayed recombination from quantum tunneling and from thermal ionization. Furthermore, nothing is known from these experiments about nature of the traps, even so the antisite defects are probable candidates. At higher temperatures, and also at room temperature, both tunneling (or even thermally assisted tunneling) and thermal ionization can be present simultaneously.

4. Conclusions

The CL experiments and analyses of scintillation decays measured in a broad time range point to rather complex behavior of garnet samples. The fit of the scintillation decays provides two components – a fast exponential term with the decay time 50–70 ns and a slow power-law dependence of the intensity $\propto t^{-p}$. The exponential decay originates from the prompt electron–hole recombination at Ce^{3+}, while the power function can be explained as tunneling-driven energy transfer process, where electrons tunnel from shallow traps towards $5d_1$ (Ce^{3+}) state where subsequently recombine. This tunneling results in undesirable slow component of the scintillation response. In the multicomponent Gd, Ga substituted garnets relative contribution of the power-law component to the overall intensity decreases and the dominant scintillation decay part is due to prompt recombination of electrons and holes at the Ce^{3+} emission centers. Consideration of the tunneling process provides a physical ground for the slower scintillation decay component in LuAG:Ce, which cannot be explained by sole thermal detrapping and recombination via conduction band.

Acknowledgments

This work was supported from the Grant Agency CR, Grant no. P204/12/0805.

References

[1] M. Nikl, A. Yoshikawa, K. Kamada, K. Nejezchleb, C.R. Stanek, J.A. Mares, K. Blazek, Prog. Cryst. Growth Charact. Mater. 59 (2013) 47.
[2] T. Martin, A. Koch, J. Synchrotron Radiat. 13 (2006) 180.
[3] J. Tous, K. Blazek, M. Kucera, M. Nikl, J.A. Mares, Radiat. Meas. 47 (2012) 311.
[4] M. Nikl, E. Mihokova, J. Pejchal, A. Vedda, Y. Zorenko, K. Nejezchleb, Phys. Status Solidi B 242 (2005) R119.
[5] Y.V. Zorenko, V.I. Gorbenko, G.B. Stryganyuk, V.N. Kolobanov, D.A. Spasskii, K. Blazek, M. Nikl, Opt. Spectrosc. 99 (2005) 923.
[6] M. Nikl, A. Vedda, M. Fasoli, I. Fontana, V.V. Laguta, E. Mihokova, J. Pejchal, J. Rosa, K. Nejezchleb, Phys. Rev. B 76 (2007) 195121.
[7] K. Kamada, T. Endo, K. Tsutumi, T. Yanagida, Y. Fujimoto, A. Fukabori, A. Yoshikawa, J. Pejchal, M. Nikl, Cryst. Growth Des. 11 (2011) 4484.
[8] K. Kamada, T. Yanagida, J. Pejchal, M. Nikl, T. Endo, K. Tsutumi, Y. Fujimoto, A. Fukabori, A. Yoshikawa, J. Phys. D: Appl. Phys. 44 (2011) 505104.
[9] E. Mihóková, K. Vávrů, K. Kamada, V. Babin, A. Yoshikawa, M. Nikl, Radiat. Meas. 56 (2013) 98.
[10] M. Kucera, K. Nitsch, M. Kubova, N. Solovieva, M. Nikl, J.A. Mares, IEEE Trans. Nucl. Sci. 55 (2008) 1201.
[11] V. Babin, V. Gorbenko, A. Makhov, J.A. Mares, M. Nikl, S. Zazubovich, Y. Zorenko, J. Lumin. 127 (2007) 384.
[12] M. Kucera, K. Nitsch, M. Nikl, M. Hanus, S. Danis, J. Cryst. Growth 312 (2010) 1538.
[13] P. Schauer, J. Bok, Nucl. Instrum., Methods Phys. Res. B 308 (2013) 68.
[14] J. Bok, P. Schauer, Meas. Sci. Technol. 25 (2014) 075601.
[15] M. Kucera, M. Nikl, M. Hanus, Z. Onderisinova, Phys. Status Solidi – Rapid Res. Lett. 7 (2013) 571.
[16] M. Kucera, M. Hanus, Z. Onderisinova, P. Prusa, A. Beitlerova, M. Nikl, IEEE Trans. Nucl. Sci. 61 (2014) 282.
[17] D.J. Robbins, B. Cockayne, B. Lent, C.N. Duckworth, J.L. Glasper, Phys. Rev. B 19 (1979) 1254.
[18] H. Ogino, A. Yoshikawa, M. Nikl, J.A. Mares, J.I. Shimoyama, K. Kishio, J. Cryst. Growth 311 (2009) 908.
[19] M. Fasoli, A. Vedda, M. Nikl, C. Jiang, B.P. Uberuaga, D.A. Andersson, K.J. McClellan, C.R. Stanek, Phys. Rev. B 84 (2011) 081102 (R).
[20] M. Tachiya, A. Mozumder, Chem. Phys. Lett. 28 (1974) 87.
[21] D.J. Huntley, J. Phys.: Cond. Matter 18 (2006) 1359.
[22] K. Brylew, W. Drozdowski, A.J. Wojtowicz, K. Kamada, A. Yoshikawa, J. Lumin. 154 (2014) 452.